

# A Low-Cost Flexible Inkjet-Printed Echo State Network for Impact Localization

S. Akter, S. K. Islam, M. R. Haider

*Dept. of EECS*

*University of Missouri-Columbia*  
Columbia, MO, USA

{shahrin.akter, mhaider}@missouri.edu

M. R. Opu, S. D. Gardner

*Dept. of ECE*

*University of Alabama at Birmingham*  
Birmingham, AL, USA

S. A. Pullano

*Dept. of Health Sciences*

*University Magna Graecia of Catanzaro*  
Catanzaro, Italy

**Abstract**—Impact localization plays a vital role in continuous monitoring of damage and fatigue testing in various healthcare applications. It is particularly important for assessing potential risk factors in spinal cord and orthopedic injuries, and in monitoring the health of athletes. Flexible sensor technology, especially the inkjet printing process on flexible substrates, is gaining significant interest due to its cost efficiency, mass production, simplicity, and environmental sustainability advantages. However, the efficiency of inkjet printed sensors is limited due to the constraints of their low-maintenance fabrication process. The integration of artificial intelligence with inkjet-printed sensors can address the limitations in their operational efficiency. In the field of artificial intelligence, Echo State Network is increasingly being implemented in a wide range of applications due to its computational simplicity. This work presents an Echo state network integrated with a tactile sensor within the network reservoir, inkjet-printed on a polyethylene terephthalate film substrate. The readout layer of the Echo State Network is constructed with multi-layer perceptrons followed by a majority voting layer. The tactile sensitivity is tested with a pencil impact experiment on different sensor surface areas. Our designed Echo State Network with an integrated tactile sensor accurately predicts the location of the pencil drop with a precision of 92.31%.

**Index Terms**—Echo state network (ESN), reservoir computing, inkjet printing, tactile sensor.

## I. INTRODUCTION

Tactile sensors are showing great promise for a variety of applications, especially in smart and IoT-enabled biomedical sensors, advanced healthcare, and industrial automation [1] [2]. In athletics or recreation-related activities, collisions or contact sports create significant risks of concussions or impact injuries, making it essential for real-time monitoring and exposure to risk assessment [3]. The widespread use of IoT devices allows for continuous, real-time monitoring and control of systems, improving automation and reliability while reducing the need for human intervention. Furthermore, the integration of artificial intelligence with these technologies is advancing, making systems more capable of real-time monitoring, classification, and prediction. Using inkjet printing to implement these technologies on flexible electronics offers additional benefits such as compactness, cost-effectiveness, and environmental sustainability, making the entire sensor ecosystem more appealing for mass production [4].

The phenomenon of miniaturization is manifest across various technological domains. As devices shrink, there is a growing need for sensors that are accurate, energy-efficient, cost-effective, and environmental friendly while still capable of mass production. Inkjet printing and flexible electronics are emerging as prevalent solutions to fulfill these requisites. Inkjet printing facilitates the fabrication of sensors on flexible substrates, yielding advantages such as reduced power consumption, lower costs, and environmental sustainability [5] [6]. Nonetheless, inkjet printing typically does not attain the same level of precision as other silicon-based technologies due to its minimal fabrication process. Fusion of inkjet printing with artificial intelligence could enhance these sensors' precision and overall functionality. This integration offers dual benefits: (1) amelioration of the accuracy limitation inherent in the inkjet printing process and (2) production of power efficient artificially intelligent sensor ecosystem.

Over the past few decades, in the realm of artificial intelligence, Reservoir Computing (RC) has demonstrated superior performance compared to other machine learning models in analyzing time series data for IoT devices. RC is a recurrent neural networks based framework which is well-suited for processing temporal or sequential signals. Among different RC methods, Echo State Network (ESN) has emerged as a prominent alternative to gradient descent-based neural networks due to its better convergence and simpler computational requirements, making it suitable for hardware implementation. Previously, through inkjet printing, neurons for a RC [6] are designed, as well as vibration and proximity sensor [7] [8], tactile sensor [9] are designed. In our work, we have designed the reservoir of ESN in the inkjet printing technology and developed a low-cost inkjet printed (IJP) tactile sensor, which is embedded in the reservoir of an ESN network to make the sensor more efficient than conventional IJP sensors.

The contents of this work are as follows. First, for preliminaries, inkjet-printing technology and ESN are introduced and explained in Section II, followed by the details of the proposed architecture in Section III. The sensor testing and data collection process is explained in Section IV, and the results are shown and discussed in Section V. Lastly, the future research plan is elaborated in Section VI and followed by a conclusion in Section VII.

## II. PRELIMINARIES

### A. Inkjet Printing Technology

The basic inkjet printing process typically involves three main steps: (1) designing the pattern using a digital editing tool, (2) printing the pattern in layers, and (3) thermally curing the printed material. Additional fabrication steps, such as plasma treatment and spin coating, may be incorporated depending on the specific research requirements. Along with additional fabrication processes, sometimes novel materials, such as graphene, hexagonal boron nitride (hBN), etc., are used in sensor printing [10].

Most inkjet printing systems utilize the Dimatix Materials Printer (DMP), which can be considerably expensive. In our research, we employed a standard drop-on-demand, piezoelectric printer (Epson XP-960) to print on polyethylene terephthalate (PET) film with a thickness of  $135\mu\text{m}$ . The silver nanoparticle ink used in this study was sourced from Mitsubishi Paper Mills Inc. (model NBSIJ-MU01). After printing, the sensor was thermally cured at a range of temperatures on a hotplate for a specified duration.

### B. Echo State Network

In RC, input data are transformed into spatiotemporal patterns within a high-dimensional space using a recurrent neural network, a process known as the reservoir. The transformed data is then analyzed for patterns in the readout layer. A key feature of RC is that the input weights and the weights of the recurrent connections within the reservoir are not trained, whereas the weights of the connections in the readout layer are trained using simple learning algorithms such as linear regression [11]. Echo State Network is a type of RC introduced by Jaeger in 2007 [12]. It has gained significant popularity within the field of RC. Fig. 1 represents the basic architecture of an ESN. It contains three layers as RC: an input layer, a reservoir layer, and an output layer, popularly known as the readout layer. Weights and biases of input and reservoir layers are denoted as  $W_{in}$  and  $W_{res}$ , respectively, and are initialized randomly and kept fixed during training. Only the reservoir to output layer connection is trainable and weights of reservoir to output connection  $W_o$  change during training. In

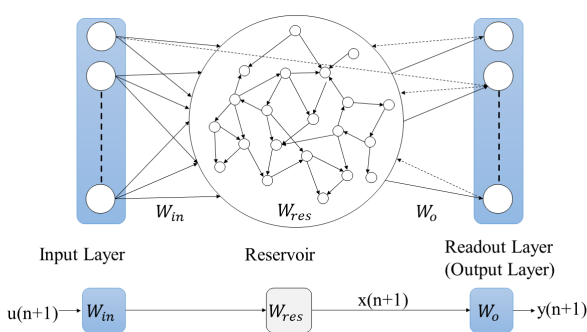


Fig. 1. Generic Structure of an Echo State Network.

the ESN, backward connection to the reservoir layer and direct connection from input to output from readout is optional, which is shown by the dotted line in Fig. 1. The reservoir state of the ESN and output update laws are defined by equations (1) and (2).

$$x(n+1) = f(W_{in}u(n+1) + W_{res}x(n)) \quad (1)$$

$$y(n+1) = W_o x(n+1) \quad (2)$$

Where  $u(n)$  indicates the input fed into the ESN,  $x(n)$  is the reservoir state, and  $y(n)$  is the output state at time  $n$ .  $W_{in}$ ,  $W_{res}$ , and  $W_o$  are the input, reservoir, and output layer weights, respectively, and  $f(\cdot)$  is the non-linear activation function. To achieve the echo state property of the reservoir weight, it needs to be scaled by spectral radius  $\lambda_{max}$ .

In a sparsely connected reservoir, 5-10% weights are nonzero, and the readout layer is trained by a simple regression method. As there is only one simple trainable layer, ESN is a low computation-intensive network. Therefore, ESN is broadly used in different areas, such as pattern recognition, time series data analysis, anomaly detection system modeling and control, etc. In the conventional ESN, the readout layer typically employs a regression method, making it a continuous-valued computation model. However, our research aims to localize the pencil-dropping area of the grid. Therefore, we have opted to use a multi-layer perceptron (MLP) in the readout layer instead of a regression method to facilitate this classification task.

## III. PROPOSED ARCHITECTURE

In our work, we have developed an ESN network where the reservoir is embedded with a tactile sensor. Our work is explained in Fig. 2. Here, an IJP tactile sensor embedded reservoir is biased with a source meter, and the sensor's sensitivity is tested with a pencil impact experiment. Multiple MLPs are used for the readout layer of the ESN network, followed by a majority voting layer.

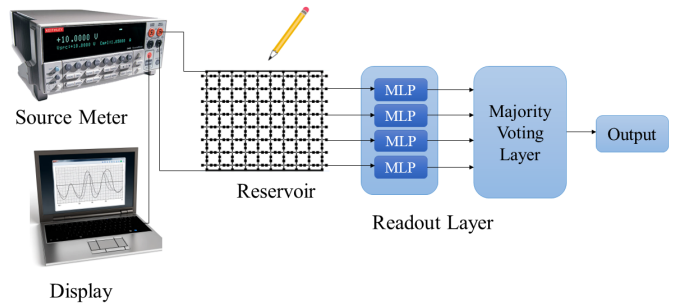


Fig. 2. Experimental setup of pencil impact experiment on a tactile sensor embedded ESN network.

### A. Reservoir Design

The reservoir of the ESN is designed by an 8X10 crossbar grid IJP on a PET film substrate with dimensions of 180 mm in length and 215 mm in width using inkjet printing. Silver

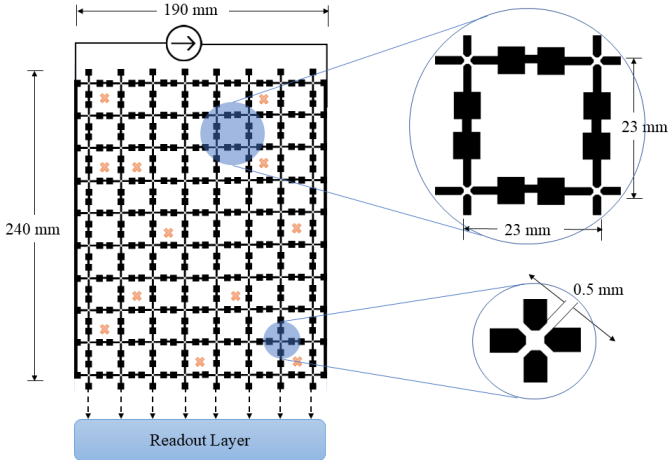


Fig. 3. Cross grid reservoir of ESN is shown with all relevant dimensions. Here, the x-mark sign indicates a randomly chosen area for pencil impact. The dotted line from the reservoir to the readout layer indicates the randomly chosen connection from the reservoir to the readout layer.

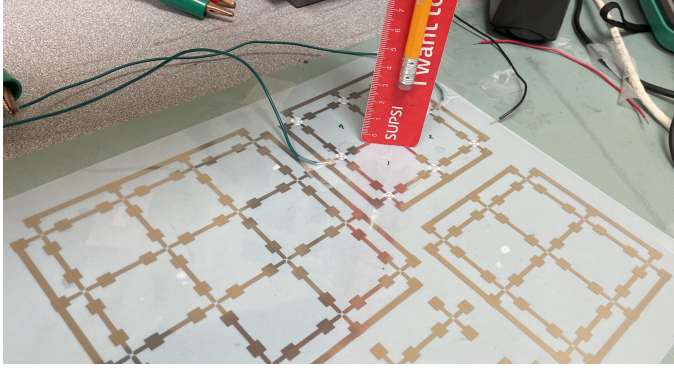


Fig. 4. Pencil drop experiment in the tactile sensor.

(Ag) ink is employed to create the reservoir pattern on the PET film. Reservoir architecture with all relevant dimensions is shown in Fig. 3. The reservoir grid is 240 mm long and 190 mm in width, with a gap of 0.5 mm at the crossing point of the grid. This gap functions as a capacitive tactile sensor and shows nonlinear voltage-current behavior. The nonlinear behavior is utilized as an activation function for each node to perform the nonlinear higher dimensional mapping of the sensor response. Two opposite sides of the grid with 10 lines are connected and used for current biasing, while the other two opposite sides with 8 lines are utilized for data collection. Among the eight lines of the grid, we randomly chose four lines to connect with the readout layer, indicating the presence of a certain number of zero values in reservoir weight.

#### B. Readout Layer Design

In a generic ESN, linear regression is typically used in the readout layer to predict continuous data points. However, since we aim to predict discrete data points associated with pencil drop events, we have opted for an MLP instead of linear

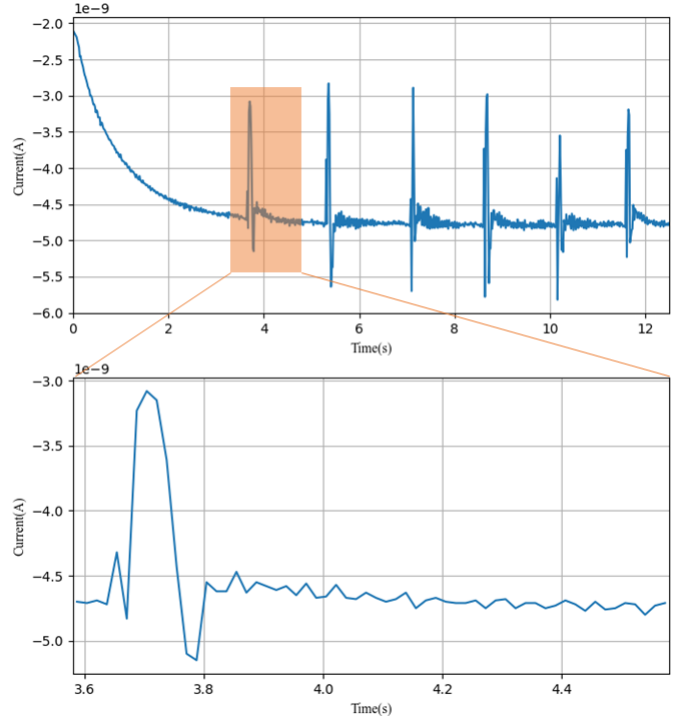


Fig. 5. Current signal for multiple pencil drops in a random point of reservoir. Each disturbance in the graph represents a pencil drop.

regression. Each connection from the reservoir to the readout layer is processed through an individual MLP. Our experiment was performed by selecting 12 random areas, dropping a pencil in each area, and recording the resulting impacts. Four random connection lines are chosen from the reservoir to readout layer connection, and each feeds to identical MLP models.

The MLP is constructed with three fully connected layers containing 500, 600, and 600 neurons, respectively. It adheres to two design principles: (1) incorporating dropout after each layer to enhance the model's generalization capabilities, and (2) using the rectified linear unit (ReLU) as the activation function to prevent gradient saturation. The network concludes with a softmax layer. The dropout rates for the input, hidden, and output layers are set at 0.1, 0.2, and 0.3, respectively. Following the MLP layers, a majority voting mechanism [13] is employed to offset the lower efficiency of the IJP reservoir since IJP sensors are lower in accuracy because of their manufacturing process.

#### IV. SENSOR TESTING AND DATA COLLECTION

Testing was conducted using a Keithley 2604B Dual channel Source Meter Unit with a Python interface. The sensor was evaluated with a current bias of 0.5 nA.

After fabrication, the sensor's effectiveness was gauged through a pencil drop test. Fig. 4 shows a pencil drop experiment in the tactile sensor. During the test, a pencil was let fall from a uniform height onto 12 spots chosen at random across the sensor grid. Out of the total lines available for gathering the test data, four were randomly selected for each pencil

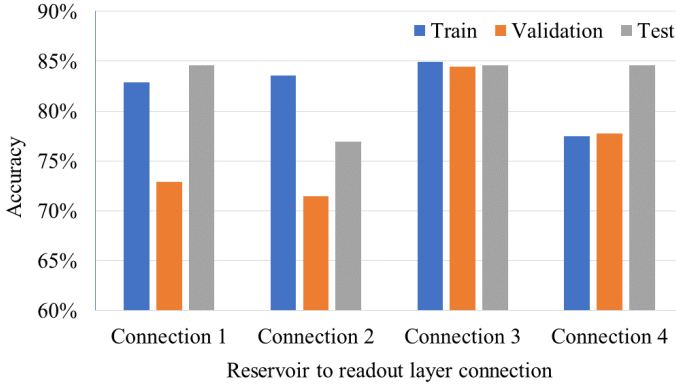


Fig. 6. Accuracy (Training, Validation, and Testing) for 4 MLPs in the readout layer.

drop to record time series data. This strategy of randomizing the selection of the drop locations and data collection lines serves multiple purposes: it helps prevent overfitting in the subsequent machine learning analysis, reduces the computational load, and cuts down on processing time. Fig. 5 depicts the current and voltage response of the sensor to each pencil impact, with the disturbances in the graph corresponding to individual drops. Post-impact, the sensor typically registers about 60 readings as it returns to equilibrium. A window-slicing technique was employed to distinguish each pencil drop incident in the current waveform. On average, each grid area was subjected to six pencil drops, resulting in a collection of 63 time series instances. This time series dataset created by current signal originated from pencil impact was then used to train and validate the machine-learning model.

## V. RESULT ANALYSIS

The time series dataset derived from the pencil impact experiment has been divided into training and testing sets at a ratio of 8:2. To compensate for the limited amount of experimental data, we employed data augmentation techniques [14] such as jittering, scaling, slicing, and wrapping on the training set. Specifically for the wrapping method, our approach included magnitude wrapping, time-invariant wrapping, window wrapping, sub-optimal wrapping, as well as guided wrapping techniques that are both random and discriminative guided wrapping. We enhanced our training dataset to include 672 samples through data augmentation. The model was trained using the Adam optimizer and the categorical cross-entropy loss function, with a learning rate set to 0.001. During training, the dataset was fitted with a 20% validation split. In Fig. 6, training, validation, and testing accuracy for all readout layer MLPs are shown, and accuracy for all MLPs is in the range of 70-85%. However, after using the majority voting layer, the overall accuracy of the model reached 92.31%. Without the use of data augmentation, there's a risk of overfitting, while the complexity of MLP models must be increased to enhance accuracy.

## VI. DISCUSSION AND FUTURE WORK

The construction of the IJP tactile sensor, integrated with the ESN, demonstrates some inconsistencies primarily due to human error, which may result in minor variations in the sensor's biasing. However, the sensor's response behavior remains consistent across all tests. During data collection, we encountered limitations in collecting data simultaneously from four lines due to restrictions in our data collection instruments. As a result, we manually simulated the same pencil drop event for each line, which may introduce slight variations in the timing and pressure applied by the pencil on the sensor.

Our future objectives include the capacity for concurrent data acquisition from all lines. Additionally, we plan to refine the design to accommodate variations in node spacing and patterns that correspond to critical pressure points. We also intend to advance the algorithm to transmit its output to devices such as phones, PCs, or other diagnostic tools for real-time impact monitoring and medical diagnosis.

## VII. CONCLUSION

In this study, a tactile sensor embedded in ESN was developed using inkjet printing technology. Using silver nanoparticle ink, a simple crossbar grid design was printed using a standard office inkjet printer onto a PET film. The IJP reservoir of the network also functioned as a tactile sensor. Data on the current flow were collected over time through a pencil impact experiment, where a pencil was dropped onto randomly chosen reservoir areas. The data from the tactile sensor-integrated reservoir was randomly delivered to the readout layer. For the readout layer, instead of using regression methods, a MLP was employed for each output neuron, followed by a majority voting layer. This random selection of data collection lines and pencil impact areas helped reduce the overfitting of the network. The results demonstrated that the majority voting layer increased the overall accuracy of the system. Integrating an IJP sensor with artificial intelligence mitigates the efficiency limitations of conventional IJP sensors. This affordable and flexible sensor is suitable for a wide range of applications, including environmental research, military surveillance, safety systems, and smart home technology. Its adaptability also makes it ideal for personalized wearable health monitors and tracking sports injuries. Flexibility allows for application in irregular surface like inside helmet depending on the relative impact force and exposures.

## ACKNOWLEDGMENT

This work was supported by the USA National Science Foundation (NSF) under Grant no. ECCS-2201447. Any opinions, findings, and conclusions or recommendations expressed in this material are those of the author(s) and do not necessarily reflect the views of the National Science Foundation.

## REFERENCES

- [1] R. S. Dahiya, G. Metta, M. Valle and G. Sandini, "Tactile Sensing—From Humans to Humanoids," in *IEEE Transactions on Robotics*, vol. 26, no. 1, pp. 1–20, Feb. 2010.

[2] G. De Maria, C. Natale, and S. Pirozzi, "Force/tactile sensor for robotic applications," *Sens. Actuators A, Phys.*, vol. 175, pp. 60–72, 2012.

[3] O'Connor, K.L., Rowson, S., Duma, S.M., Broglio, S.P., "Head-Impact-Measurement Devices: A Systematic Review," *Journal of Athletic Training*, vol. 52, no. 3, pp. 206–227, 2017.

[4] M. R. Opu, S. D. Gardner and M. R. Haider, "A Low-Cost Inkjet-Printed Heart Sound Sensor for Telehealth Application," 2023 IEEE 66th International Midwest Symposium on Circuits and Systems (MWSCAS), Tempe, AZ, USA.

[5] S. Gardner, A. Porbanderwala and M. R. Haider, "An Affordable Inkjet-Printed Foot Sole Sensor and Machine Learning for Telehealth Devices," *IEEE Sensors Letters*, vol. 7, no. 6, pp. 1–4, June 2023.

[6] S. D. Gardner and M. R. Haider, "An Inkjet-Printed Artificial Neuron for Physical Reservoir Computing," *IEEE Journal on Flexible Electronics*, vol. 1, no. 3, pp. 185–193, July 2022.

[7] S. D. Gardner, M. R. Opu and M. R. Haider, "An Inkjet-Printed Capacitive Sensor for Ultra-Low-Power Proximity and Vibration Detection," 2023 IEEE Wireless and Microwave Technology Conference (WAMICON), Melbourne, FL, USA, 2023, pp. 73–76.

[8] S. D. Gardner, J. I. D. Alexander, Y. Massoud and M. R. Haider, "Minimally produced inkjet-printed tactile sensor model for improved data reliability," 2020 11th International Conference on Electrical and Computer Engineering (ICECE), Dhaka, Bangladesh.

[9] T. Yun, S. Eom, and S. Lim, "Paper-based capacitive touchpad using home inkjet printer," *Journal of Display Technology*, vol. 12, no. 11, pp. 1411–1416, 2016.

[10] R. F. Hossain and A. B. Kaul, "Inkjet-printed MoS<sub>2</sub>-based field-effect transistors with graphene and hexagonal boron nitride inks," *J. Vac. Sci. Technol. B*, vol. 38, no. 4, p. 42206, Jul. 2020.

[11] G. Tanaka, T. Yamane, J. B. Héroux, et al. "Recent advances in physical reservoir computing: A review," *Neural Networks*, vol. 115, p. 100–123, 2019.

[12] H. Jaeger, "The 'echo state' approach to analysing and training recurrent neural networks-with an erratum note," German Nat. Res. Center Inf. Technol., Karlsruhe, Germany, GMD Tech. Rep. 148, 2001, p. 34.

[13] A. Dogan and D. Birant, "A Weighted Majority Voting Ensemble Approach for Classification," 2019 4th International Conference on Computer Science and Engineering (UBMK), Samsun, Turkey.

[14] B. K. Iwana and S. Uchida, "An empirical survey of data augmentation for time series classification with neural networks," *PLoS ONE*, vol. 16, no. 7, Jul. 2021.